Molecular Microbiology (2006) **59**(5), 1576–1590

doi:10.1111/j.1365-2958.2006.05041.x
First published online 20 January 2006

GTP drives myosin light chain 1 interaction with the class V myosin Myo2 IQ motifs via a Sec2 RabGEF-mediated pathway

Pamela Bielli,[1,2] Elena Caroli Casavola,[1] Antonino Biroccio,[3] Andrea Urbani[4,5] and Antonella Ragnini-Wilson[1*†]

[1]*Department of Biology, University of 'Tor Vergata' Rome, Viale Della Ricerca Scientifica, 00133-Rome, Italy.*
[2]*Department of Developmental and Cellular Biology, University 'La Sapienza', Rome, Italy.*
[3]*Clinical Biochemistry Laboratory, Children's Hospital Bambin Gesù – IRCCS, Rome (Vatican State), Piazza San Onofrio 4, Rome 00166, Italy.*
[4]*Centro Studi sull'Invecchiamento (Ce.S.I.), Fondazione Università 'G. D'Annunzio', Chieti, Italy.*
[5]*Dipartimento di Scienze Biomediche, Università 'G. D'Annunzio' di Chieti e Pescara, Italy.*

Summary

The yeast myosin light chain 1 (Mlc1p) belongs to a branch of the calmodulin superfamily and is essential for vesicle delivery at the mother-bud neck during cytokinesis due to is ability to bind to the IQ motifs of the class V myosin Myo2p. While calcium binding to calmodulin promotes binding/release from the MyoV IQ motifs, Mlc1p is unable to bind calcium and the mechanism of its interaction with target motifs has not been clarified. The presence of Mlc1p in a complex with the Rab/Ypt Sec4p and with Myo2p suggests a role for Mlc1p in regulating Myo2p cargo binding/release by responding to the activation of Rab/Ypt proteins. Here we show that GTP or GTPγS potently stimulate Mlc1p interaction with Myo2p IQ motifs. The C-terminus of the Rab/Ypt GEF Sec2p, but not Sec4p activation, is essential for this interaction. Interestingly, overexpression of constitutively activated Ypt32p, a Rab/Ypt protein that acts upstream of Sec4p, stimulates Mlc1p/Myo2p interaction similarly to GTP although a block of Ypt32 GTP binding does not completely abolish the GTP-mediated Mlc1p/Myo2p interaction. We propose that Mlc1p/Myo2p interaction is stimulated by a signal that requires Sec2p and activation of Ypt32p.

Accepted 14 December, 2005. *For correspondence. E-mail antonella.ragnini@uniroma2.it; Tel. (+39) 0872 570317; Fax (+39) 0872 570412. †Present address: Department of Cell Biology and Oncology, Consorzio Mario Via Nazionale, 66030 Santa Maria Imbaro (CH), Italy.

Introduction

Class V myosin interaction with cargo membranes is required for the short-range axonal/dendridic transport of secretory vesicles at nerve terminals and synapses, for the polarized transport of organelles in pigmented cells, as well as for polarized growth and cell separation in yeast. Human dysfunctions such as Griscelli syndrome and related syndromes arise from a defect in the binding of cargo to class V myosin (Seabra and Coudrier, 2004). In mammals, vesicle/organelle class V myosin anchoring requires the activation of the vesicle/organelle-associated Rab/Ypt small GTPases. Rab/Ypt protein activation, by promoting the recruitment of accessory factors that act as bridging proteins, allow vesicle/organelle binding to the C-terminus of the class V myosin motor (Goud, 2002; Hales *et al*., 2002; Wu *et al*., 2002; Fehrenbacher *et al*., 2003).

Class V myosin-mediated transport in mammalian cells is also regulated by binding of calcium/calmodulin to their IQ motifs (Bahler and Rhoads, 2002). Recent structural studies have shown that changes in calcium levels cause calmodulin to be bound or released from myosin V IQ motifs with consequent changes in the conformation of the myosin V structure that also affect the cargo binding domain (Krementsov *et al*., 2004; Li *et al*., 2004; Wang *et al*., 2004).

Although budding yeast possess all the components of the vesicle-motor anchoring machinery, and an interaction between the class V myosin Myo2p and the Rab/Ypt Sec4p is required for secretory vesicle transport to the sites of vesicle delivery during budding and mating (Wagner *et al*., 2002; Pruyne *et al*., 2004), there has been no demonstration so far that Rab/Ypt protein activation or calcium/calmodulin regulates this process. Myo2p interacts with another essential myosin light chain, Mlc1p, in addition to calmodulin. Mlc1p is essential for viability and for secretory vesicle delivery at the mother-bud neck during cytokinesis (Stevens and Davis, 1998; Wagner *et al*., 2002). Like calmodulin, the essential function of Mlc1p

resides in its ability to bind to IQ motifs present in target proteins but, by having abortive EF hand motifs, it is unable to bind calcium (May *et al*., 1997; Terrak *et al*., 2003).

Mlc1p and calmodulin possess a dumbbell-shaped structure with EF hand motifs located in the N- and C-terminal globular domains that are connected by a flexible linker region (Terrak *et al*., 2003). This structure allows these proteins to interact with IQ motifs either in an extended conformation, in which only one globular domain interacts with an IQ motif, or as a compact structure, in which both the N-terminal and the C-terminal domains interact with the IQ motifs. It has been postulated that Mlc1p or calmodulin might interact with multiple targets in their open conformation. Thus, the switch from the compact to the extended conformation appears to be important for regulating the interaction of this class of proteins with target motifs (Bahler and Rhoads, 2002; Krementsov *et al*., 2004; Li *et al*., 2004; Wang *et al*., 2004). The signal that controls the conformational switch of Mlc1p remains unclear (Terrak *et al*., 2003).

Myo2p, Sec4p and its GDP/GTP exchange factor (GEF) Sec2p are essential for vesicle anchoring and motility during vegetative growth and mating (Walworth *et al*., 1989; Johnston *et al*., 1991; Walch-Solimena *et al*., 1997; Schott *et al*., 1999). Mlc1p overexpression suppresses the growth defects caused by poor prenylation of Rab/Ypt (Bialek-Wyrzykowska *et al*., 2000). In addition to class V myosin IQ motifs, Mlc1p binds in a regulated manner to the IQ motifs of the class II myosin Myo1p and acts as a receptor for the IQGAP-like protein Iqg1/Cyk1. This latter event occurs just before cytokinesis, and the presence of Iqg1/Cyk1 at the mother-bud neck promotes the recruitment of actin filaments to the Myo1p ring and actomyosin ring contraction (Boyne *et al*., 2000; Shannon and Li, 2000). After actomyosin ring contraction and the disappearance of Myo1p and Iqg1p from the mother-bud neck, Mlc1p colocalizes with secretory vesicles and Sec2p at the mother-bud neck until cell separation. Thermosensitive *mlc1* mutants are defective in both vesicle delivery to the centre of the mother-bud neck and actomyosin contraction. Taken together, these data indicate that Mlc1p has a particular role in regulating the events that lead to secretory vesicle delivery at the mother-bud neck during cytokinesis (Wagner *et al*., 2002).

How Mlc1p, Sec2p and Sec4p act in controlling Myo2p-mediated vesicle delivery at the mother-bud neck during cytokinesis remains to be established. Although genetic and biochemical evidence have shown that Sec4p and Sec2p recruitment on vesicle membranes is essential for vesicle transport (Walch-Solimena *et al*., 1997; Elkind *et al*., 2000), direct evidence that Sec4p activation by GTP binding is required for Myo2p recruitment onto vesicle membranes is still missing.

Sec4p activation requires Sec2p membrane binding which depends partially on determinants located in its C-terminus and partially on its ability to interact with either of two redundant Rab/Ypt proteins, Ypt31p or Ypt32p (Ortiz *et al*., 2002). Ypt31p/32p localize to *trans*-Golgi membranes and recycling vesicles (Jedd *et al*., 1997) and have a function in protein recycling between the plasma membrane, endosomes and the Golgi compartment (Chen *et al*., 2005). *In vitro* binding studies show that they interact preferentially with Sec2p when in a GTP-bound state, although GDP binding does not completely abolish this interaction. The role of Ypt31p/32p and Sec2p interaction remains unclear, but it has been suggested that it might be a prerequisite for Sec4p activation and thus for Sec4p interaction with the Exocyst component Sec15p (Ortiz *et al*., 2002).

To determine whether Rab/Ypt protein activation plays a role in promoting Mlc1p/Myo2p interaction, we have studied the effects of GTP and Sec4p or Ypt31p/32p activation in the formation of the Mlc1p/Myo2p complex. Here we report data consistent with a role of GTP and/or Ypt32p activation, but not Sec4p activation, in stimulating Mlc1p and Myo2p IQ motif interaction via a pathway that requires Sec2p membrane binding.

Results

Mlc1p interaction with IQ motifs is stimulated and/or stabilized by the addition of GTP or GTPγS to cell extracts

The signal that stimulates Mlc1p interaction with target IQ motifs is unknown (Terrak *et al*., 2003). To study whether small G protein activation may have a role in promoting Mlc1p and Myo2p interaction, we employed a widely used approach that relies on the high affinity of small G proteins for guanine nucleotides. The addition of GTP, GTPγS or GDP to cell extracts drives the small G proteins to their GTP- (active) or GDP- (inactive) bound state according to the guanine nucleotide added in excess (Walworth *et al*., 1989; Feig, 1999; Gao *et al*., 2003). This approach has been shown to be a powerful method to study the composition of the complexes formed upon small G protein activation in cell extracts (Collins *et al*., 1997; Walch-Solimena *et al*., 1997; Feig, 1999; Elkind *et al*., 2000; Ortiz *et al*., 2002).

Unless otherwise indicated, the following experiments were performed using cell extracts from wild-type (wt) cells or secretory mutant (*sec*) cells that expressed a fully functional green fluorescent protein (GFP)-tagged Mlc1 protein (GFPMlc1p) from a centromeric plasmid (Wagner *et al*., 2002). GFPMlc1p was immunoprecipitated from detergent solubilized cell extracts (Grote *et al*., 2000) with an anti-GFP antibody (αGFP) in the presence of 5 mM GTP, GTPγS or GDP or without the addition of any

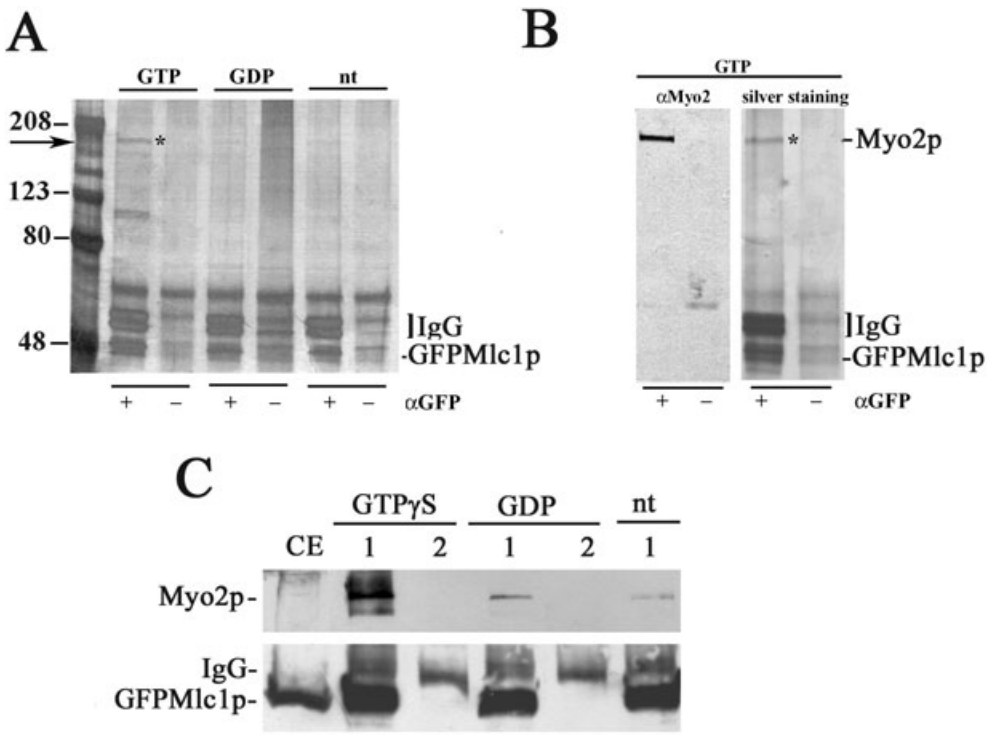

Fig. 1. GFPMlc1p/Myo2p complex formation is stimulated upon GTP, but not GDP, addition to wt crude extracts in a manner that does not require GTP hydrolysis.
A. Silver staining of a 6% SDS-polyacrylamide gel of immunoprecipitates (IP) obtained with anti-GFP antibody (αGFP) from cell extracts of wt cells (K699) expressing GFPMlc1p centromeric plasmid (Mlc1pUG34) and treated with 5 mM GTP (panel GTP), 5 mM GDP (panel GDP) or no nucleotides (panel nt). Lanes + and – indicate the samples to which αGFP was added or not respectively. The band of 181 kDa that corresponds to Myo2p (after analysis by MS-MALDI-TOF, see also Fig. S1) is indicated by an arrow and asterisk. The numbers on the left of the panel indicate the position of the molecular weight markers (Bio-Rad pre-stained).
B. αGFP immunoprecipitates from GTP-treated crude extracts (as in A) were run in parallel on 6% SDS-polyacrylamide gels and immunoblotted with the anti-Myo2p antibody (left) or silver-stained (right). The band corresponding to Myo2p is labelled and indicated by an asterisk in the right panel. Lanes + and – indicate the samples to which αGFP was added or not respectively.
C. Crude extracts from wt cells (K699) expressing Mlc1pUG34 treated with 5 mM GTPγS, 5 mM GDP or no nucleotides (nt) were immunoprecipitated with the αGFP (1) or α-HIS as a mock reaction (2). IP reactions were separated by 10% SDS-PAGE, blotted and immunodetection was performed using either the αMyo2p or the αGFP antibody (to detect GFPMlc1p). (CE: 60 μg of crude extract were loaded: 2.5 mg of CE was used in each IP reaction). The bands corresponding with GFPMlc1p and Myo2p are indicated. IgG, immunoglobulin G.

guanine nucleotide. As controls, immunoprecipitation (IP) reactions were carried out in parallel either by omitting αGFP in the IP buffer, by using cell extracts from cells expressing the GFP protein alone or by using as mock reaction α-HIS. The proteins present in the αGFP immunoprecipitates were separated by SDS-PAGE and analysed quantitatively by silver staining followed by mass spectroscopy and MALDI-TOF analysis of the band of interest, or qualitatively by immunoblot analysis using an anti-Myo2p antibody.

Silver staining of the αGFP immunoprecipitates prepared from wt (K699) cell extracts expressing Mlc1GFP in the presence of GTP highlighted a band of about 181 kDa (band indicated by the arrow in Fig. 1A, panels GTP) corresponding to the molecular weight of Myo2p. A similar band was weakly visible in GDP- or no nucleotide-treated samples (Fig. 1A, panels GDP and nt respectively), and absent in the control samples (omission of the antibody, Fig. 1A, lanes –) or when the GFP was expressed alone (Fig. S1). MALDI-TOF-recorded monoisotopic masses of tryptic peptides obtained from the band with an apparent mobility of about 181 kDa in silver stained gels (Fig. S1) showed overlaps with the expected theoretical mass of Myo2p (NCBI Accession No. 6324902) with a confidence greater than 95% ($P < 0.05$) with respect to a randomly occurring assignment. Immunoblot analysis using an anti-Myo2p antibody confirmed that the 181 kDa band corresponded to Myo2p (Fig. 1B and C). The 181 kDa band was also present in the αGFP pull-down of GTPγS-treated cell extracts (Fig. S1). Immunoprecipitates from GTPγS-, GDP- or no nucleotide-treated samples analysed and quantified by immunoblot analysis confirmed the pattern observed by silver staining: the amount of the Mlc1p/Myo2p complex present in GTPγS-treated samples is sig-

Table 1. *Saccharomyces cerevisiae* strains used in this study.

Name	Genotype	Source
K699	*MAT*a *leu2-3112 ura3 his3-11,15 trp1-1 ade2-1 can1-100*	K. Nasmyth
AR9-13A	*MAT*a *leu2 ura3 his3 trp1* ***sec2-59***	Wagner *et al*. (2002)
RSY22	*MAT*α *leu2-3112 ura3-1 his3-11,15 trp1-1 ade2-loc can1-100* ***myo2Δ6IQ***	Stevens and Davis (1998)
RSY271	*MAT*α *ura3-52 his4-619* ***sec18-1***	R. Schekman
WWY116-7D[a]	*MAT*α *leu2-3112 ura3-1 his3-11,15 trp1-1 ade2-loc* ***sec4-8***	Wagner *et al*. (2002)
YER031C	MATα *leu2Δ0, ura3Δ0 his3Δ1 lys2Δ0* ***YER031c::kanMX4*** (Δ*ypt31*)	EUROFAN ID16583 BY4742

a. K699 isogenic strains.
All *sec* mutant strains are complemented by the respective wt protein expressed from centromeric plasmids. Bold face indicates relevant mutant alleles.

nificantly higher compared with GDP-treated or untreated samples (Fig. 1C; the quantification data are given in Fig. S1).

Mlc1p/Myo2 complex formation upon GTP stimulation occurs via the Myo2p IQ motifs

The analyses described above show that silver staining provides an easy and reproducible way to simultaneously control the amount of proteins present in different IP samples and to detect the differences in the amounts of the Mlc1p/Myo2p complex in treated, untreated and control samples, so we chose this technique followed by MS-MALDI-TOF analysis of the band of interest (when necessary) to screen a panel of secretion and myosin mutants described below.

To determine whether Mlc1p/Myo2p interaction occurs via the Myo2p IQ motifs, we performed experiments similar to those described above using extracts prepared from wt and *myo2Δ6IQ* cells (Table 1). The *myo2Δ6IQ* strain expresses a mutant Myo2p that is not expected to interact with Mlc1p due to the absence of the six IQ motifs present in Myo2p (Stevens and Davis, 1998). The *myo2Δ6IQ* strain does not show significant growth defects (Schott *et al*., 2002), and while Mlc1p localization at the bud tip is somewhat reduced in this strain, the bud-neck localization remains unaffected (Shannon and Li, 2000).

Two proteins with an apparent molecular mass of 224 kDa and 181 kDa specifically co-immunoprecipitated with GFPMlc1p in GTP-treated samples from wt cells (Fig. 2, band 1 and band 2 respectively). Only one protein with a mobility that was intermediate between band 1 and band 2 was specifically immunoprecipitated by the αGFP antibody in GTP-treated samples of the *myo2Δ6IQ* strain (Fig. 2, band 3).

The MALDI-TOF recorded monoisotopic masses of the tryptic peptides obtained from the wt band 2 (181 kDa protein) overlaps with the expected theoretical mass of the class V myosin Myo2p, with a confidence greater than 95% ($P < 0.05$) with respect to a randomly occurring assignment (band 2, Fig. S2). The peptide finger print of the wt band 1 (band 1, Fig. S2) fitted the class II myosin Myo1p (molecular weight 224 297 Da). The band observed in the IP from the *myo2Δ6IQ* extract (Fig. 2, band 3) has a tryptic peptide mass fingerprint that fits with that of the class II myosin Myo1p (NCBI Accession No. 6321812) with a confidence score greater than 95% ($P < 0.05$; band 3, Fig. S2). Being beyond the scope of this work, the reasons for the faster mobility of Myo1p in *myo2Δ6IQ* compared with the wt Myo1 protein or the reason of the occasional presence of the Myo1p/Mlc1p complex in the GTP-treated extracts of wt was not further investigated.

In summary, we conclude that GTP or GTPγS addition to crude extracts from wt cells expressing GFP-Mlc1p potently stimulates the formation and/or stabilization of

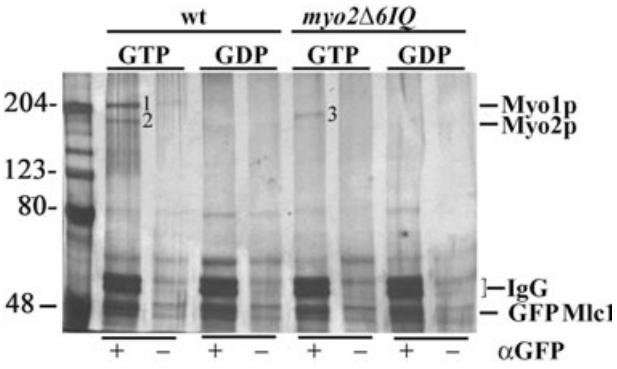

Fig. 2. GTP promotes Mlc1p interaction with Myo2 IQ motifs. Silver staining of a 6% SDS-polyacrylamide gel of immunoprecipitates of αGFP IP reactions obtained from crude extracts of wt (K699) or *myo2Δ6IQ* (RSY22) cells carrying the Mlc1pUG34 plasmid treated with 5 mM GTP (lanes GTP) or 5 mM GDP (lanes GDP). The nature of band 1, band 2 and band 3 (indicated with the numbers 1, 2 and 3, respectively, in figure) was determined, as indicated in the text, by MS-MALDI-TOF analysis. The tryptic peptides of band 1 fitted with a confidence score greater than 95% ($P < 0.05$) accuracy with the *S. cerevisiae* class II myosin Myo1p (NCBI Accession No. 6321812). The tryptic peptides obtained from band 2 overlapped with that of the Myo2p (NCBI Accession No. 6324902) with a confidence greater than 95% ($P < 0.05$) with respect to a randomly occurring assignment. The tryptic peptides of the *myo2Δ6IQ* band 3 fitted with a confidence score greater than 95% ($P < 0.05$) accuracy with the *S. cerevisiae* class II myosin Myo1 protein. The peptide coverage and further details of the MALDI-TOF analysis of these bands are given in Fig. S2. The position of the Myo1p and Myo2p band in the wt GTP-treated samples, and the GFPMlc1p bands are indicated. The numbers on the left of the panel indicate the position of the molecular weight markers (Bio-Rad pre-stained). IgG, immunoglobulin G.

the Mlc1p/Myo2p complex and that this interaction occurs via the IQ motifs of Myo2p.

GTP promotes Mlc1p/Myo2p IQ motif interaction and/or stabilization via a pathway that requires the Sec2p C-terminus

We reported previously that Mlc1p associates with secretory vesicles in a complex with the Rab/Ypt Sec4p and/or Myo2p (Wagner *et al*., 2002). We reasoned that Sec2p, by acting as GEF for the Rab/Ypt protein Sec4p (Walch-Solimena *et al*., 1997; Elkind *et al*., 2000), might be an intermediary in the GTP signal that leads to Mlc1p/Myo2p complex formation. The *sec2-59* mutant encodes Sec2$^{1\text{-}374aa}$p that lacks the C-terminal domain that is required for Sec2p membrane binding. This defect results in the accumulation of secretory vesicles in the mother cell body, possibly by a defect in linking secretory vesicles to the vesicle transport motor machinery or by an inability of Sec2$^{1\text{-}374aa}$p to reach its target, Sec4p, at the vesicle membrane (Walch-Solimena *et al*., 1997). Importantly, however, Sec2$^{1\text{-}374aa}$p is still able to interact with the wt or the nucleotide-free form of the Rab/Ypt Sec4p (Sec4^{N133I}p; Ortiz *et al*., 2002) but, like the wt Sec2p, does not interact with the dominant-active Sec4 GTP-bound form (Sec4p^{Q79L}p; Walch-Solimena *et al*., 1997).

The ability of GTP to stimulate Mlc1p/Myo2p interaction in wt or *sec2-59* cells expressing GFPMlc1p was tested in cultures shifted from 25°C to 37°C for 1 h and 30 min. This time point was chosen because it is well known that actin cytoskeleton polarization is affected by this temperature shift such that actin filaments depolarize within 10 min of the shift and repolarize after 1 h and 20 min due to the activation of a morphogenetic checkpoint (Lew, 2000). Detergent-solubilized cell extracts were used for IP experiments and the amount of the Myo2p/Mlc1p complex present in 5 mM GTP-treated samples was visualized by silver staining (Fig. S3) or analysed by immunoblot analysis using the anti-Myo2p antibody (Fig. 3).

Myo2p was found in the αGFP pull-down from wt cells (Fig. 3A, *K699/GFPMlc1*, lane +) but not in the *sec2-59* αGFP pull-down (Fig. 3A, *sec2-59*/GFPMlc1, lane +) or when the αGFP antibody were omitted (Fig. 3A, lanes –). Expression of the Sec2HA protein from an ectopic plasmid in the *sec2-59* mutant fully restores the GTP-mediated Mlc1p/Myo2p complex formation/stabilization (Fig. 3A, lanes *sec2-59/GFPMlc1/Sec2HA*).

As this result could also be due to a lower amount of

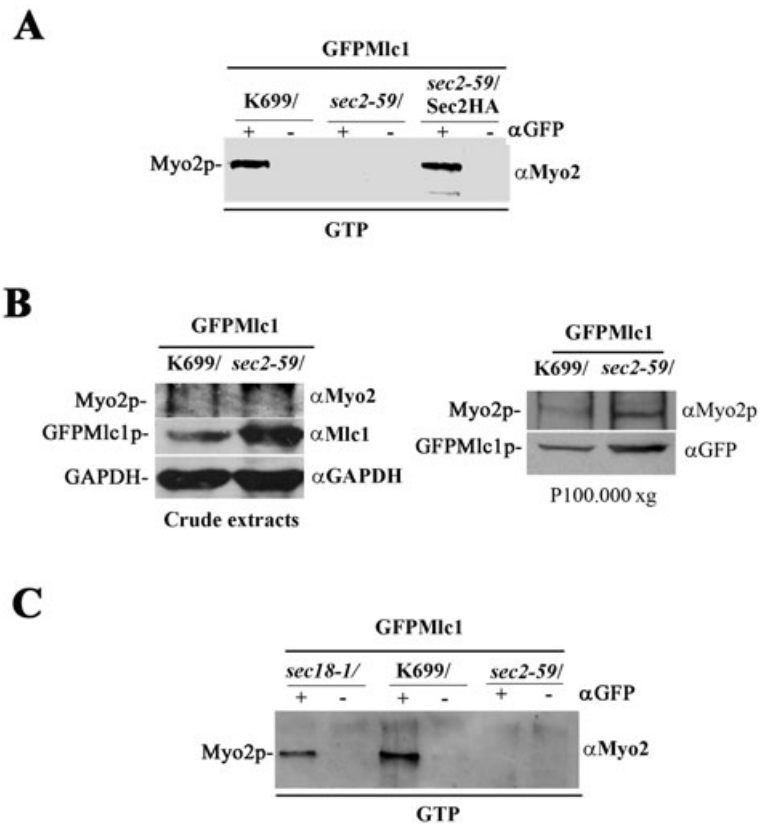

Fig. 3. GTP promotes Mlc1p/Myo2p interaction and/or stabilization via a pathway that requires the Sec2p C-terminus.
A. Immunoblot analysis of the IP reactions obtained with αGFP from 5 mM GTP-treated cell extracts of wt cells (K699), *sec2-59* (AR9-13A) and *sec2-59* transformed with a Sec2p-HA-expressing plasmid. All strains expressed GFPMlc1p. Cells were incubated at 28°C and then shifted for 1 h and 30 min to 37°C before cell extract preparation. αGFP IP reactions of the indicated strains were loaded onto a 6% SDS-polyacrylamide gel and analysed by immunoblotting with the anti-Myo2p antibody (or by silver staining, Fig. S3). Lanes + and – indicate the samples to which the αGFP was added or not respectively.
B. Left: Crude extracts (50 μg) obtained from wt cells (K699) and *sec2-59* cells were separated by 8.5% SDS-PAGE and immunoblot analysis was performed with the indicated antibody. Right: P100.000 *xg* detergent-solubilized fractions were prepared from crude extracts using the same strains indicated in (A). Detergent solubilized proteins (60 μg) obtained from the P100.000 *xg* fractions were separated by 8.5% SDS-PAGE and immunoblot analysis was performed with the indicated antibody.
C. Immunoblot analysis (and silver staining, Fig. S3) of the IP reactions obtained with αGFP from 5 mM GTP-treated cell extracts of wt (K699), *sec2-59* (AR9-13A) or *sec18*-1 (RSY271) cells expressing GFPMlc1p (Mlc1pUG34). Following separation the gel was blotted and immunodetection was performed using the αMyo2p antibody. Lanes + and lanes – indicate the samples to which anti-GFP antibody (αGFP) was added or not respectively.

Myo2p and/or GFPMlc1p in the *sec2-59* cells compared with wt cells, the amounts of these proteins in the crude extracts was determined by immunoblot analysis. We observed that while the amount of GFPMlc1p or of the glycolytic enzyme glyceraldehyde-3-phosphate dehydrogenase (GAPDH) of *Saccharomyces cerevisiae* (Miaczynska *et al*., 1997) is comparable in the wt and *sec2-59* cell extracts, little or no Myo2p was detected in the same samples (Fig. 3B, left). The difficulty of detecting Myo2p in wt crude extracts by Western blot analysis was previously reported (Reck-Peterson *et al*., 1999) and is due to the fact that Myo2p co-fractionates with high-speed membranes (P100.000 *xg*). Thus, we prepared the P100.000 *xg* fractions from crude extracts obtained from the above strains by differential centrifugation (see *Experimental procedures*). After detergent solubilization of the membranes (Grote and Novick, 1999), the amount of Myo2p in these samples was determined by immunoblot analysis using αMyo2 and αGFP was used to detect the GFPMlc1 protein (Fig. 3B, right). Comparable amounts of Myo2p were present in both samples. Therefore, the absence of Myo2p in the *sec2-59* GTP-treated pull-down experiment was not due to differential expression of Myo2p or Mlc1p but to the defect in the Sec2 protein.

Finally, to rule out the possibility that a block in vesicle transport could non-specifically interfere with the GTP-induced Mlc1p/Myo2p complex formation/stabilization, the IP assays were repeated using cell extracts from *sec18-1* cells cultured in parallel with wt or *sec2-59* cells (Fig. 3C). The *sec18-1* strain was chosen because the *SEC18* gene encodes the yeast *N*-ethylmaleimide-sensitive factor-like protein (NSF) which is required for vesicle docking and fusion at all stages of vesicle transport. A shift of *sec18-1* cells to 37°C results in a generalized block of vesicle transport at a stage downstream of Rab/Ypt activation (Graham and Emr, 1991; Grote *et al*., 2000). We observed that Myo2p co-immunoprecipitates with GFPMlc1p in GTP-treated samples of both wt and *sec18-1* cells, but not in GTP-treated samples of *sec2-59* cells (Fig. 3C and Fig. S3). This implicates Sec2p specifically in the process of Mlc1p/Myo2p complex formation.

In summary, the data presented thus far show that GTP and GTPγS stimulate the formation and/or stabilization of the Mlc1p/Myo2p complex, that this interaction occurs via the IQ motifs of the Myo2p and that it requires the C-terminus of Sec2p.

A block of Sec4p activation does not interfere either with Mlc1p/Myo2p binding or with the formation of the Sec4p/Myo2p complex

As mentioned above, the $Sec2^{1\text{-}374aa}$ protein, encoded by the *sec2-59* allele, retains the ability to bind Sec4pGDP or nucleotide-free Sec4p and is able to act as a Sec4p-GEF but is unable to reach its target on membranes due to the absence of the C-terminal domain that is required for membrane binding (Walch-Solimena *et al*., 1997; Elkind *et al*., 2000). Despite extensive analysis, it is not yet clear whether the *sec2-59* mutant arrests growth at the restrictive temperature because of a defect in activation of the membrane-bound Sec4p or because there is another function associated with the C-terminus and/or its ability to bind membranes (Walch-Solimena *et al*., 1997; Elkind *et al*., 2000; Ortiz *et al*., 2002). To discriminate between which of these scenarios might affect the ability of GTP to stimulate Mlc1p/Myo2p interaction and/or complex stabilization in a *sec2-59* background, we analysed the effects of GTP-stimulated co-IP of Myo2p with Mlc1p using different Sec4p mutations.

For these tests we used a thermosensitive Sec4p mutant, *sec4-8* (encoding the GTP binding-defective $Sec4^{G147D}$p), which affects not only the ability of Sec4p to bind GTP but also its structure as the $Sec4^{G147D}$ protein is not recognized by the anti-Sec4p antibody (Walworth *et al*., 1989; Jedd *et al*., 1997; Mulholland *et al*., 1997). In a second set of experiments, we used cell extracts obtained from cells expressing the dominant-negative Sec4 proteins $Sec4^{S34N}$ and $Sec4^{N133I}$ and compared their effects on Mlc1p/Myo2p complex formation with cells expressing the dominant-active $Sec4^{Q79L}$ allele. $Sec4^{S34N}p$ accommodates GDP but assumes a conformation that cannot be recognized by the RabGDI (Collins *et al*., 1997), a protein that solubilizes GDP-bound Rab/Ypt proteins from membranes (Pfeffer *et al*., 1995). $Sec4^{N133I}p$ remains preferentially in a guanine nucleotide-free state. $Sec4^{Q79L}p$ locks Sec4p in its GTP-bound conformation (Walworth *et al*., 1989; Collins *et al*., 1997; Grote and Novick, 1999).

Wild-type and mutant *sec4-8* cells were incubated in parallel and then shifted to the restrictive temperature for 1 h and 40 min before testing the ability of Myo2p to co-immunoprecipitate with GFPMlc1p in the presence of GTP. Cells expressing the dominant negative ($Sec4^{S34N}$ and $Sec4^{N133I}$) and the dominant-active ($Sec4^{Q79L}$) Sec4p versions were shifted to galactose-containing medium and the cells were harvested when GFPMlc1p had polarized at the incipient bud site or bud tip (see *Experimental procedures*; Wagner *et al*., 2002).

The band corresponding to Myo2p was visible in GTP-treated samples of αGFP IPs from wt and *sec4-8* cells (Fig. 4A, *sec4-8* and wt lanes +) but not, as expected, from those samples obtained from *sec2-59* cells (Fig. 4A, *sec2-59* lanes +) or when the αGFP antibody was omitted from the IP reactions (Fig. 4A, lanes –). A band corresponding to Myo2p was also visible in the IPs of cells expressing dominant-negative $Sec4^{S34N}$ and $Sec4^{N133I}$ mutants as well as in those expressing the dominant-active $Sec4^{Q79L}$ or wt

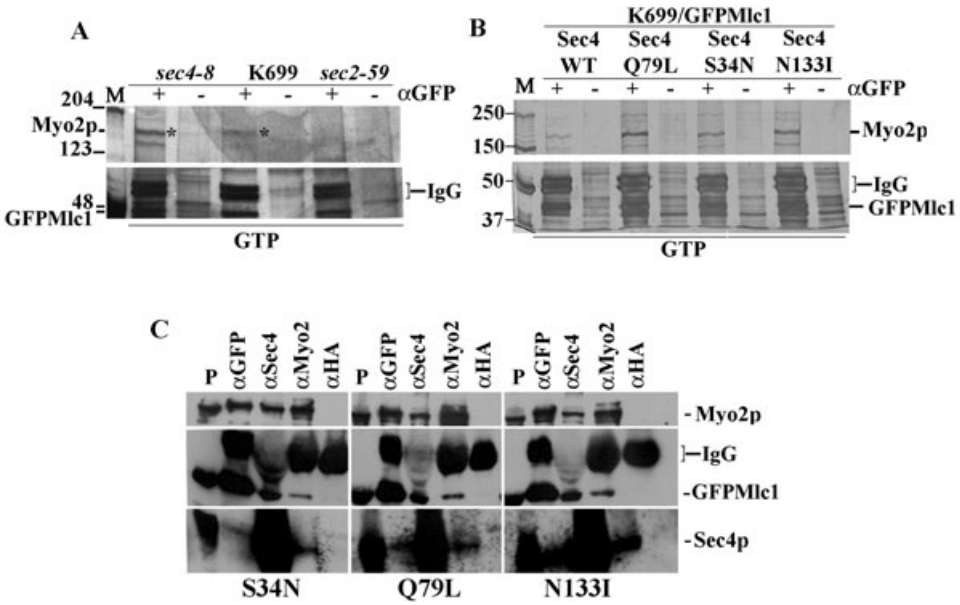

Fig. 4. GTP-promoted Mlc1p/Myo2p interaction does not require Sec4p activation.
A. Protein extracts from *sec4-8* (WWY116-7D; *sec4-8* lanes), wt (K699 lanes) or *sec2-59* (AR9-13A; *sec2-59* lanes) cells expressing GFPMlc1p were immunoprecipitated with the anti-GFP antibody (αGFP) in the presence of 5 mM GTP. The immunoprecipitates were separated by 6% SDS-polyacrylamide gel and analysed by silver staining. The Myo2p band is labelled and indicated with an asterisk. The position of the GFPMlc1p band is also shown. Molecular weight markers (M) are shown on the left. IgG, immunoglobulin G.
B. Wild-type cells overexpressing GFPMlc1p from the pUG34 plasmid and the wt Sec4p (Sec4pYES2; Sec4WT panel) or the mutant Sec4p versions – $Sec4^{S34N}$ ($Sec4^{S34N}$pYES2; Sec4S34N panel), $Sec4^{Q79N}$ ($Sec4^{Q79L}$pYES2; Sec4Q79L panel), $Sec4^{N133I}$ ($Sec4^{N133I}$pYES2; Sec4N133I panel) – expressed from a Gal1/10 promoter were grown in glucose medium, shifted to galactose-containing medium (to $OD_{600} = 0.8$) and harvested when the cells had polarized GFPMlc1p at the sites of bud growth. Then the crude extract was prepared, treated with 5 mM GTP and immunoprecipitated as in (A). The IP pellets were separated on a 6% SDS-polyacrylamide gel and then silver staining was performed. The Myo2p band and GFPMlc1p band are indicated. Molecular weight markers (M) are shown on the left. IgG, immunoglobulin G.
C. Sec4p activation is not required for Sec4p interaction with Myo2p on vesicle membranes. Detergent-solubilized P100.000 *xg* vesicle-enriched membranes (lanes P) were obtained from wt cells overexpressing GFPMlc1p and the $Sec4^{S34N}$ ($Sec4^{S34N}$pYES2; panel S34N), $Sec4^{Q79N}$ ($Sec4^{Q79L}$pYES2; panel Q79L) or $Sec4^{N133I}$ ($Sec4^{N133I}$pYES2; panel N133I) mutants. Immunoprecipitation of the proteins was performed by using αGFP, αSec4, αMyo2 or, as a negative control, αHA antibody. The IP pellets were loaded onto a 12.5% SDS-polyacrylamide gel and in the immunoblot analysis αMyo2, αGFP or αSec4 antibody was used. The band corresponding to each protein is indicated. IgG, immunoglobulin G.

Sec4p (Fig. 4B, respective lanes +) but not in the respective controls (Fig. 4B, lanes –). Thus, defects in Sec4p GTP binding do not alter the ability of GTP to stimulate Mlc1p/Myo2p interaction and/or complex stabilization.

As mentioned previously, although is clear that Sec4p, Myo2p and Mlc1p are part of a complex when associated with secretory vesicles (Wagner *et al.*, 2002), it had not been established whether Sec4p GTP binding is required to allow Sec4p interaction with Myo2p on vesicle membranes. We therefore tested the possibility that Mlc1p/Myo2p interaction with Sec4p might be altered by defects in Sec4p GTP binding.

For this we prepared high-speed vesicle fractions (the P100.000 *xg* fraction of cell extracts) from cells expressing *$Sec4^{S34N}$p*, *$Sec4^{N133I}$p*, *$Sec4^{Q39L}$p* and GFPMlc1p. After a shift to galactose the cells were grown for the time required for cells expressing the mutant Sec4p to polarize GFPMlc1p to the incipient bud site and bud tip.

Co-immunoprecipitation was carried out by using detergent solubilized P100.000 *xg* membranes incubated with anti-Sec4p, anti-Myo2p or anti-GFP antibody (to immunoprecipitate the GFPMlc1p) or, as a mock reaction, with an anti-HA antibody. As shown in Fig. 4C, expression of dominant-negative Sec4p (*$Sec4^{S34N}$p* or *$Sec4^{N133I}$p*) or dominant-active $Sec4^{Q39L}$p does not alter the ability of Sec4p/Myo2p/Mlc1p to co-immunoprecipitate together from P100.000 *xg* high-speed vesicle membrane fractions.

From these data we conclude that an inability of Sec4p to bind GTP does not influence either the ability of Mlc1p to bind to Myo2p in response to GTP addition to cell extracts or the ability of Sec4p to bind to the Mlc1p/Myo2p complex.

Ypt32 activation promotes Mlc1p/Myo2p interaction and/or complex stabilization in a manner similar to GTP addition to cell extracts

The picture that emerges from the above studies suggests that a function exerted by the Sec2p C-terminus (possibly

the function that this domain has in Sec2p membrane recruitment) underlies the mechanism by which GTP and GTPγS promote Mlc1p/Myo2p interaction or complex stabilization. One possibility is that Sec2p might act as a membrane-bound GTP-sensitive factor that stimulates the formation of the Mlc1p/Myo2p complex by promoting the recruitment of Myo2p to vesicle membranes in response to the activation of an upstream GTPase.

It was previously shown that Ypt31/32 protein activation plays a role in Sec2p recruitment onto membranes. Ypt32p or Ypt31p overexpression rescues the *sec2-59* growth defect, possibly by promoting the membrane anchoring of the otherwise cytosolic $Sec2^{1\text{-}374aa}$ protein encoded by the *sec2-59* allele (Ortiz *et al*., 2002). If Sec2p membrane binding is required for GTP-stimulated Mlc1p/Myo2p complex formation/stabilization, then the effect of GTP addition might be reciprocated by activated Ypt31p/32p.

We therefore tested whether expression of a dominant-active Ypt32 mutant ($Ypt32^{Q72L}$) promotes Mlc1p/Myo2p interaction similarly to GTP addition to cell extracts. For these studies we used strains expressing GFPMlc1p but lacking Ypt31 (Δ*ypt31* cells) due to the redundancy of Ypt31p and Ypt32p (Jedd *et al*., 1997). As a negative control we expressed the dominant-negative Ypt32 mutant ($Ypt32^{S27N}$) in the Δ*ypt31* background. The $Ypt32^{Q72L}$ mutant protein has a lower rate of GTP hydrolysis compared with the wt Ypt32p protein while the $Ypt32^{S27N}$ protein preferentially binds GDP (Walworth *et al*., 1989; Collins *et al*., 1997; Ortiz *et al*., 2002).

Both $Ypt32^{Q72L}$ or the dominant negative $Ypt32^{S27N}$ protein were expressed under a Gal1/10 promoter. After overnight growth in glucose, the $Ypt32^{S27N}$ Δ*ypt31* and the $Ypt32^{Q72L}$ Δ*ypt31* cells were shifted to galactose and harvested when GFPMlc1p was still polarized at the sites of bud growth. GFPMlc1p was then immunoprecipitated in the presence or absence of 5 mM GTP with the αGFP antibody or as a mock reaction by adding only Protein A Sepharose beads. After SDS-PAGE separation of the IP samples, silver staining (Fig. 5A, left) or immunoblot analyses was carried out as described above using αMyo2p (Fig. 5A, right).

A clear difference in the amount of Myo2p co-immunoprecipitated with GFPMlc1p was observed in untreated IP samples of $Ypt32^{Q72L}$ compared with $Ypt32^{S27N}$ (Fig. 5A; Ypt32Q72L, Ypt32S27N, lanes nt). Quantification of the amount of Myo2p immunoprecipitated by αGFP (Fig. 5B) shows that about 50% more Myo2p was found in the pull-down reactions obtained from cells expressing the $Ypt32^{Q72L}$ than from those expressing $Ypt32^{S27N}$.

Surprisingly, however, we observed that in GTP-treated samples of either $Ypt32^{Q72L}$ or $Ypt32^{S27N}$ mutant extracts the Myo2p/Mlc1p complex did not differ significantly in the amount of Myo2p that was co-immunoprecipitated (Fig. 5; Ypt32Q72L, Ypt32S27N, lanes GTP). Therefore, inhibition of Ypt32-GTP binding is not sufficient to block the ability of GTP to stimulate Mlc1p/Myo2p complex formation/stabilization. This latter finding suggests that an additional GTP-sensitive factor acts in promoting Mlc1p/Myo2p interaction/stabilization via a Sec2p dependent pathway. In summary, Ypt32p activation mimics *in vivo* the effect of GTP addition to cell extracts by stimulating Mlc1p/Myo2p complex formation/stabilization. However, inactive Ypt32p is not sufficient to abolish the ability of GTP to stimulate Mlc1p/Myo2p interaction *in vivo*, in contrast to the deletion of the Sec2p C-terminus.

We conclude that Ypt32p is one of the GTPases involved in the GTP signal that stimulates the interaction/stabilization of the Mlc1p/Myo2p complex via the Sec2p. However, in addition to Ypt32p, another GTP-sensitive factor must exist that acts through Sec2p in this pathway.

Sec2p is required for GFPMlc1p localization in a ring-like structure at the mother-bud neck

Mlc1p is required for secretory vesicle targeting to the centre of the septum due to its ability to interact with the IQ motifs of Myo2p (Wagner *et al*., 2002). Thus, if activation of Ypt32p promotes Sec2p recruitment onto vesicle membranes (Ortiz *et al*., 2002) and this in turn stimulates Myo2p/Mlc1p complex formation/stabilization, then we might expect that defects such as those carried by the *sec2-59* mutant would result in Sec4p, Myo2p and/or Mlc1p mislocalization at the mother-bud neck.

Indeed, this has previously been shown for Myo2p and Sec4p (Walch-Solimena *et al*., 1997; Reck-Peterson *et al*., 1999; Elkind *et al*., 2000). Furthermore, it was demonstrated that Sec2p localization at the mother-bud neck depends only partially on the role that Myo2p has in transporting secretory vesicles. In fact, it has been observed that the Myo2p mutant *myo2-2* affected solely in vacuolar transport is defective in Sec2p localization at the bud tip and mother-bud neck (Catlett *et al*., 2000; Elkind *et al*., 2000).

We showed previously that GFPMlc1p localization at the bud tip is severely affected in *sec4-8*, *sec2-59*, *sec18-1* or myosin (*myo2-66*) mutants. In addition, Sec2p mislocalizes in *mlc1 ts* mutants: Sec2p-containing vesicles accumulate at the sides of the mother-bud neck upon a shift to the restrictive temperature (Wagner *et al*., 2002). Consistent with this finding, Luo *et al*. (2004) recently reported that GFPMlc1 localization at the bud tip was indeed altered in the *sec2-41* mutant. However, they noticed that GFPMlc1p could still accumulate at the mother-bud neck in this mutant (Luo *et al*., 2004). To clarify this point, we investigated the localization of GFPMlc1p at the mother-bud neck of *sec2-59* and *sec18-1* cells after a shift to 37°C.

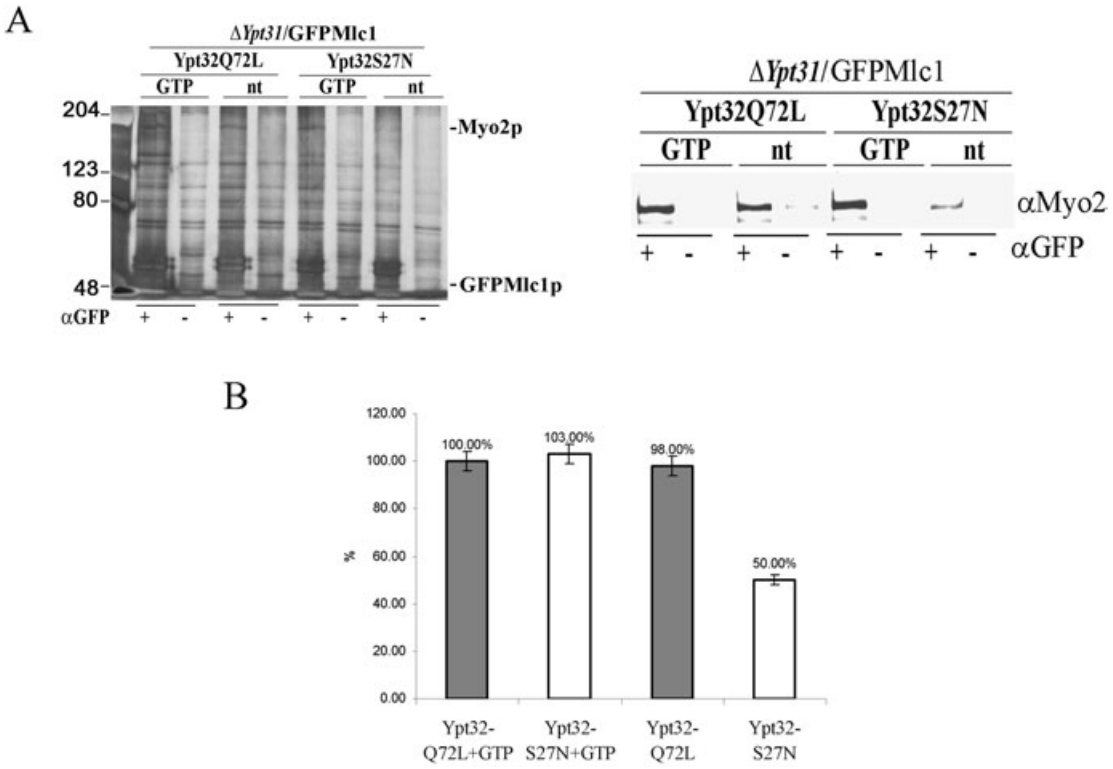

Fig. 5. Ypt32p activation stimulates Mlc1p/Myo2p interaction and/or complex stabilization in a manner similar to GTP addition to cell extracts.
A. The Δ*ypt31* (YER031C) strain transformed with a plasmid expressing GFPMlc1p from the MET3 promoter of the pUG34 plasmid (panel Δ*Ypt31*/GFPMlc1) and expressing the Ypt32^{Q72L} (lane Ypt32Q72L) or Ypt32^{S27N} (lane Ypt32S27N) proteins from the Gal1/10 promoter of the pYES2 vector was grown in glucose-containing medium before washing with sterile water and then shifted to medium supplemented with 4% galactose. Cells were harvested when GFPMlc1p showed a polarized localization at the bud tip. Immunoprecipitation from crude extracts obtained from these cultures was performed with αGFP (lanes +) in the presence of GTP (lanes GTP) or without guanine nucleotide (lanes nt) as described in the text. The immunoprecipitates were separated on a 6% SDS-polyacrylamide gel and silver-stained (left) or blotted and immunodetected with the anti-Myo2p antibody (right). Lanes – indicate the samples to which anti-GFP antibody was added or not respectively.
B. Quantification of the immunoblot in (A), showing the amount of Myo2p immunoprecipitated after expression of Ypt32^{Q72L} or Ypt32^{S27N}, as indicated, in the presence of GTP (+GTP) (filled column) or without nucleotide addition (unfilled column). The amount of Myo2p is given relative to Ypt32^{S27N} +GTP, which was arbitrarily set at 100%.

We observed that while GFPMlc1p is found in a ring-like structure at the mother-bud neck of wt cells incubated at 37°C for 1 h and 30 min (Fig. 6, panel K699), similar structures could not be seen in either *sec2-59* or *sec18-1* mutants at the restrictive temperature. Typically, soon after the shift to 37°C of the *sec2-59* mutant, GFPMlc1 accumulates as a single dot or as multiple dots located at one or both sides of the mother-bud neck or it shows diffuse fluorescence. Over 90% of the cells show abnormal localization of GFPMlc1p at the mother-bud neck after 1 h and 30 min at 37°C (Fig. 6, *sec2-59* and wt panel respectively). In *sec18-1* cells, as we reported previously, GFPMlc1p rapidly disappears from the bud tip and the mother-bud neck within 5 min from the shift (Wagner *et al*., 2002). Prolonged incubation of *sec18-1* cells at 37°C (1 h and 30 min at 37°C) causes GFPMlc1p to accumulate in internal globular structures (Fig. 6, panel *sec18-1*). Normal localization was observed in all strains at the permissive temperature (data not shown).

These observations are in agreement with what we previously observed by studying GFPMlc1p localization and motility in *sec18-1*, *sec2-59* and *sec4-8* cells (Wagner *et al*., 2002). The apparent discrepancy between our data and those reported by Luo *et al*. (2004) are simply due to the fact that Luo *et al*. (2004) considered any cell with a GFPMlc1p signal at the mother-bud neck to be positive without taking into consideration whether the protein was properly localized at this site (meaning in a ring-like structure surrounding the mother-bud neck) or simply accumulated there in an abnormal fashion (E. Bi, pers. comm.), a fact that we have considered in our study.

Thus, summarizing our data and those of Luo *et al*. (2004) it can be concluded that *sec2* mutations cause the disappearance of GFPMlc1p from the bud tip and an abnormal localization at the mother-bud neck where it is found as single or multiple dots located at the sides of the mother-bud neck rather then in a ring-like structure as in wt cells. These observations support the idea that Sec2p

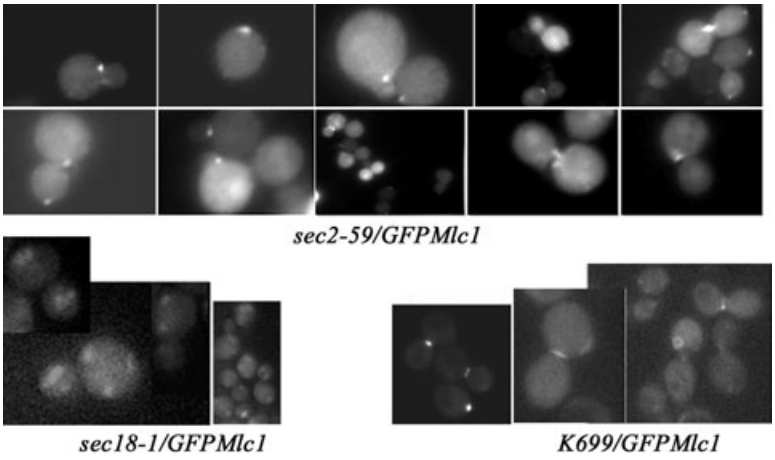

Fig. 6. GFPMlc1p localization in wt, *sec2-59* and *sec18-1* cells. GFPMlc1p localization in wt cells (K699) or *sec2-59* (AR9-13A) or *sec18*-1 (RSY271) expressing GFPMlc1p (Mlc1pUG34) grown for 1 h and 30 min at 37°C.

has a function in promoting Mlc1p assembly with target proteins at the mother-bud neck.

To corroborate the existence of a functional relationship among Sec2p, Mlc1p and Ypt32p, we determined the genetic interactions between these genes. We chose to study the effects of Mlc1p and Ypt32p coexpression in *sec2-59* cells over other possible combinations because any observed effect on growth could be more directly related to the effect that Ypt32p, Mlc1p and Sec2p have on promoting vesicle targeting to plasma membranes.

As described previously (Ortiz *et al*., 2002), Ypt32p overexpression was sufficient to allow sec2-59 cells to grow at 33°C. We observed that the coexpression of Mlc1p together with Ypt32p had a negative effect on *sec2-59* growth at 33°C. Coexpression of these two proteins does not alter the growth of wt cells at this temperature or at 25°C (Fig. 7). Mlc1p overexpression does not have any phenotype in wt, *sec* or *myo2* mutant (Shannon and Li, 2000; Wagner *et al*., 2002; Luo *et al*., 2004).

Thus, we conclude that specific genetic interactions exist between Mlc1p, Ypt32p and Sec2p. The antagonistic effects of Ypt32p overexpression versus Ypt32p and

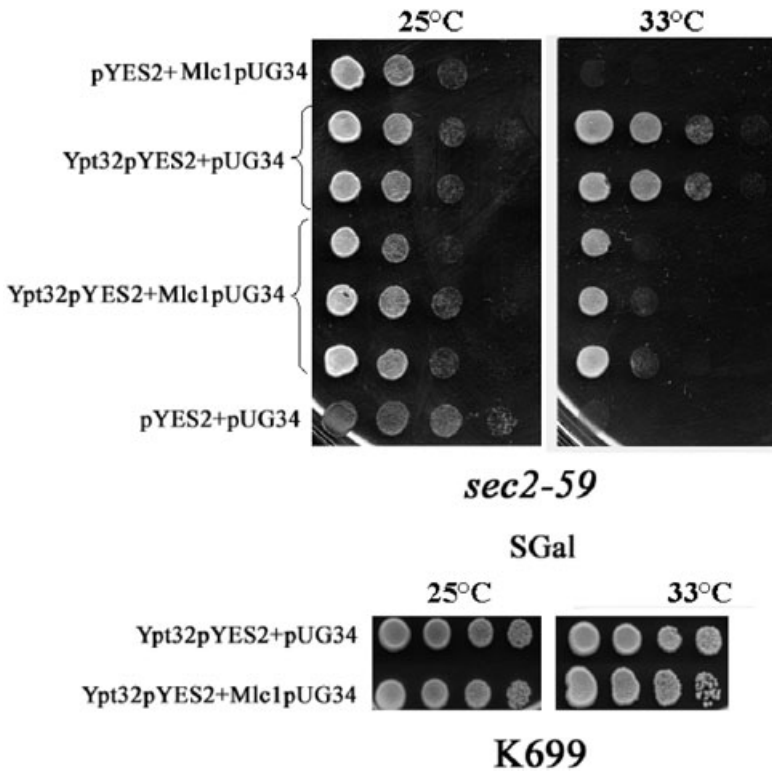

Fig. 7. Genetic interaction of YPT32 and MLC1 in secretion mutants. K699 or *sec2-59* cells (strain WWY114-4A) were transformed with YPT32pYES2 (under control of a GAL promoter) and MLC1pUG34 plasmids or with the respective empty vectors (pYES2, pUG34) as indicated in the figure. Transformants were spotted onto synthetic media supplemented with 4% galactose and lacking of uracyl and histidine to select the respective plasmids and express the YPT32p from the Gal1/10 promoter. Shown are fivefold serial dilutions of transformed strains incubated at the permissive temperature (25°C) and non-permissive temperature (33°C). Two independently isolated colonies were tested for the case of YPT32pYES2+pUG34 and three clones in the case of YPT32pYES+MLC1pUG34.

Mlc1p coexpression on *sec2-59* growth could be caused by an ability of Mlc1p to counteract the ability of Ypt32p to recruit Sec2p on vesicle membranes or by a function that Mlc1p has downstream of this complex formation.

Discussion

The yeast myosin light chain Mlc1p and its *Schizosaccharomyces pombe* homologue Cdc4p, unlike calmodulin, can not bind calcium due to mutation of their EF hand motifs (McCollum *et al*., 1995; May *et al*., 1997; Terrak *et al*., 2003). It has thus been unclear which signal stimulates the interaction of Mlc1p with target proteins. In this study we have shown that GTP or GTPγS, which are known to activate small G proteins when added to cell extracts (Feig, 1999), potently promote and/or stabilize Mlc1p interaction with Myo2p IQ motifs. Importantly, we also show that this effect is mediated via a function exerted by the C-terminus of Sec2p. In addition, we identified Ypt32p as one of the small G proteins that when activated can stimulate Mlc1p/Myo2p complex formation and/or stabilization.

Expression of dominant-active *Ypt32*^{Q72L} from an ectopic high-copy-number plasmid in Δ*ypt31* cells promotes Mlc1p and Myo2p interaction/stabilization in a manner similar to that observed upon addition of GTP to wt cell extracts. However, it is also clear that Ypt32p (and possibly Ypt31p) activation is not the only signal able to stimulate Mlc1p/Myo2p interaction/stabilization as overexpression of a dominant inactive form of the Ypt32 protein does not impair GTP-stimulated Mlc1p/Myo2p complex formation/stabilization. We interpret these data as an ability of Ypt32-GTP to act as an activator of Mlc1p/Myo2p interaction and/or complex stabilization, but Ypt32p GDP binding does not negatively regulate the formation of this complex. Sec2p appears to be a more crucial player in this process. At least one other factor (as yet unknown) acting upstream of Sec2p and sensitive to GTP must exist. Indeed, it has been observed that Sec2p binds membranes via a determinant located in its C-terminus (Elkind *et al*., 2000) via Ypt32/31 activation (Ortiz *et al*., 2002), but also by interacting with ELP1 (Rahl *et al*., 2005), a member of a six-subunit complex (named Elongator) found to co-purify with the hyperphosphorylated form of RNA polymerase II (Otero *et al*., 1999; Li *et al*., 2001). Thus, it may be possible that this latter factor may play a role in the GTP- and Sec2p-mediated Mlc1p/Myo2p complex formation/stabilization.

In this study we ruled out the possibility that Sec4p activation is required to stimulate Mlc1p/Myo2p interaction upon GTP addition to cell extracts, nor is it required for Myo2p/Sec4p interaction. Indeed, the Sec4^{S34N} and Sec4^{N133I} dominant-negative forms tightly bind their GEF, Sec2p (Walworth *et al*., 1989; Grote and Novick, 1999), in a manner analogous to the Ras^{S17N} mutant (Feig, 1999). Thus, the fact that the GTP-mediated signal leading to Mlc1p/Myo2p complex formation/stabilization is not impaired by expression of Sec4^{S34N} or Sec4^{N133I} reinforces the idea that Sec2p recruitment to vesicle membranes, and not Sec2 GEF activity, is the essential step required for the GTP-mediated Mlc1p/Myo2p interaction.

The novel finding reported here is that GTP added to cell extracts acts as a stimulus for Mlc1p/Myo2p complex formation/stabilization via a pathway that requires the Sec2p C-terminus. This finding opens the way to further characterize the mechanism of action of GTP-sensitive factors of different types that act on Sec2p membrane recruitment and on the role that such an event has for the subsequent step of exocytosis.

How might Ypt31p/32p activation mechanistically promote Mlc1p/Myo2p interaction by recruiting Sec2p to vesicle membranes?

Our data are consistent with the idea that Sec2p recruitment onto membranes upon GTP stimulation, possibly favoured by Ypt32-GTP binding, is an essential step for Mlc1p/Myo2p complex formation/stabilization. These data, together with the observation that Ypt31/32 proteins and Myo2p interact in a two-hybrid assay (Pruyne *et al*., 2004; A. Ragnini, unpubl. results), suggest that Ypt32p and Sec2p might operate in stimulating the formation/stabilization of the Mlc1p/Myo2p complex by physically interacting with each other. A more detailed analysis of the composition and time of formation of Ypt32p-, Sec2p- and Mlc1p-containing complexes in the presence or absence of GTP and in different *sec2* and *ypt32* mutant backgrounds is required to further clarify this point.

Finally, what is the final output of the GTP signal that stimulates Mlc1p/Myo2p interaction? The antagonistic effects of Mlc1p and Ypt32p overexpression in the *sec2-59* mutant suggests that there is a tightly regulated balance of the amounts of Ypt32p, Sec2p and Mlc1p expressed in the cell and their regulated interaction plays a role in favouring secretory vesicle anchoring to or release from Myo2p.

We previously showed that Mlc1p associates with Myo2p and the Sec4p on secretory vesicles and that defects in Mlc1p function cause accumulation of Sec2p-containing vesicles at the sides of the mother-bud neck (Wagner *et al*., 2002). It is tempting to speculate that Ypt32p activation, by stimulating Mlc1p/Myo2p complex formation, might act in favouring incoming secretory vesicle delivery at the mother-bud neck before and during actomyosin ring contraction.

VerPlank and Li (2005) have recently reported that Exocyst mutants are defective in contractile ring dynamics. They are able to initiate contraction but often fail to complete it due to premature disassembly of this structure that collapses at one side of the mother-bud neck. It has been

suggested that this is due to a defect in anchoring the actomyosin ring to the secretory vesicle. Interestingly, they show that the Myo1p rings (to which Mlc1p is certainly associated at this stage of the cell cycle; Boyne *et al*., 2000; Shannon and Li, 2000; Wagner *et al*., 2002) remain visible in Exocyst mutants as a dot or spots located at one or other side of the mother-bud neck, a picture that is strongly reminiscent of what is observed for GFPMlc1p localization in *sec2-59* mutants. Another possibility is that Ypt32p activation causes the resolution of the Sec4p/Myo2p/Mlc1p complex at the plasma membrane. The closest Ypt32p/Ypt31p homologue in mammals, the Rab11 protein, is known to function in delivery of membranes to the furrow. Rab11p binds to the mammalian class V myosin homologue myosin Vb via FIP proteins, and Rab11p activation is essential for plasma membrane expansion of the associated furrow ingression and/or during the abscission and separation of daughter cells. Activation of a plasma membrane-located small GTPase ARF6 is required for Rab11p-FIP3p or Rab11p-FIP4p recruitment at the furrow (Fielding *et al*., 2005).

Given the structural and functional conservation among the yeast and mammalian ARF proteins, Ypt31p/Ypt32p and Rab11p and class V myosin motors, it appears possible that the co-ordinated activation of multiple and differently regulated GTPases might be required for controlling anchoring/release of secretory vesicles before and during actomyosin ring contraction.

Experimental procedures

Plasmid construction

Plasmids and oligonucleotide primers used for PCR amplification are listed in Table 2 and Table S1 respectively. Unless indicated otherwise, PCR was performed using W303 *S. cerevisiae* genomic DNA. The plasmids *Ypt32S27N*pYES2, *Ypt32Q72LpYES2*, *Sec4*pYES2, *Sec4S34N*pYES2, *Sec4Q79L*pYES2 and *Sec4N133I*pYES2 were generated by site-directed mutagenesis using an overlap extension PCR strategy (Aiyar *et al*., 1996) and the respective oligonucleotides indicated in Table S1 to amplify BamHI–SalI (750 bp) and BamH1–Xho1 (692 bp) fragments. The fragments were then cloned into BamHI–XhoI restriction sites of the pYES2 vector. After cloning, wt and mutant alleles were sequenced (Genelab c/o ENEA Casaccia, Italy). The *Sec2HApVTU* plasmid was cloned by amplifying a Sec2 fragment (2280 bp) with the primers (#10, #11) indicated in Table S1, and digesting the PCR product with SpeI and PstI and ligating it to the pVTU-101 vector which derived from digestion of pVTU-COT1HA (kindly provided by J. Stadler) with XbaI and PstI. The Sec2HAp, Sec4p and Sec4Q79Lp expressed by the *Sec2HA*pVTU, *Sec4p*YES2 *Sec4Q79L*pYES2 plasmids were proven to fully complement the thermosensitive growth defect of the respective *ts* mutant strains (AR9-13A for the *sec2-59* mutant allele and WWY116-7D for *sec4-8*).

Strains, growth conditions, genetic and recombinant DNA methods

The yeast strains used are listed in Table 1. Yeast and bacterial media preparations and all standard yeast and *Escherichia coli* DNA isolation and manipulations, PCR reactions and transformations were performed as described previously (Bialek-Wyrzykowska *et al*., 2000; Wagner *et al*., 2002). *E. coli* cells were grown in Luria broth (LB) medium at 37°C. Yeast cells were grown at 28°C in synthetic selective media containing 2% glucose (SD) or 4% galactose (SGal) with the appropriate amino acids, unless otherwise specified.

For crude extract preparations and IP experiments with wt and *myo2Δ6IQ* cells, the respective strains were transformed with the plasmids indicated in the text or with the relevant empty vectors (pYES2, pUG34, pUG36) in order to test all strains in parallel in the same type of media. Typically, cultures were grown overnight in SD media supplemented with the appropriate amino acids to select for the relevant plasmid at 28°C and harvested at $OD_{600} = 0.8–1.0$. For temperature shift analysis, the wt, *sec2-59*, *sec18-1* and *sec4-8* strains transformed with Mlc1pUG34 (or Mlc1pUG36 when appropriate) were grown at 28°C to $OD_{600} = 0.4–0.7$ in appropriate SD medium. The cells were then pelleted by centrifugation and the pellets were resuspended in fresh pre-warmed (37°C) SD medium supplemented with the appropriate amino

Table 2. Plasmids used in this study.

Plasmid	Characteristics	Reference or source	Oligonucleotide primers used for PCR
pUG34	CEN6/ARSH4, HIS3, yEGFP3 under *MET25* promoter	J.H. Hegemann	
pUG36	CEN6/ARSH4, URA3, yEGFP3 under *MET25* promoter	J.H. Hegemann	
Mlc1pUG34	CEN6/ARSH4, HIS3, yEGFP3-MLC1 under *MET25* promoter	Wagner *et al*. (2002)	
Mlc1pUG36	CEN6/ARSH4, URA3, yEGFP3-MLC1 under *MET25* promoter	Wagner *et al*. (2002)	
Ypt32pYES2	2μ, URA3, YPT32 under *GAL1/10* promoter	This work	1, 2
Ypt32S27NpYES2	2μ, URA3, *ypt32S27N* under *GAL1/10* promoter	This work	1, 2, 3
Ypt32Q72LpYES2	2μ, URA3, *ypt32Q72L* under *GAL1/10* promoter	This work	1, 2, 4
Sec4pYES2	2μ, URA3, SEC4 under *GAL1/10* promoter	This work	5, 6
Sec4Q79L pYES2	2μ, URA3, *sec4Q79L* under *GAL1/10* promoter	This work	5, 8, 6
Sec4S34N pYES2	2μ, URA3, *sec4S34N* under *GAL1/10* promoter	This work	5, 7, 6
Sec4N133I pYES2	2μ, URA3, *sec4N133* under *GAL1/10* promoter	This work	5, 9, 6
Sec2HApVTU	2μ, URA3, *Sec2HA*	This work	10, 11

acid and incubated at 37°C for 1 h and 30 min before crude extract preparation and analysis.

The expression from the Gal1/10 promoter of the Sec4 mutant proteins (WT, Q79L, S34N and N133I) or Ypt32 proteins (Q72L and S27N) cloned in pYES plasmids was performed as follows: K699 cells transformed with Mlc1pUG34 and the respective Sec4 plasmids or Ypt32 plasmid were grown overnight at 28°C in SD medium lacking uracil and histidine. Cells were harvested at 6000 r.p.m., washed with sterile water, centrifuged, and resuspended at $OD_{600} = 0.6–0.7$ in SD medium lacking uracil and histidine and supplemented with 4% galactose. The cells were incubated at 28°C until GFPMlc1p started to polarize at the incipient bud site and/or bud tip (12–20 h). In stationary cells the GFPMlc1p signal appears depolarized in the mother cell body while in exponential phase cells GFPMlc1p polarizes at the sites of membrane growth (Wagner *et al*., 2002).

Crude extract preparation and crude extract fractionation

Briefly, after harvesting, the cell pellet was washed in 0.02% NaN_3, centrifuged, and the cell lysates used for IP and fractionation experiments were prepared as previously described (Wagner *et al*., 2002) using the glass beads method in 7 ml of lysis buffer [0.1 M Tris-HCl pH 8, 20% glycerol, 1 mM PMSF and 1 tablet of PIM (Amersham)]. The P100.000 *xg* high-speed vesicle-enriched membranes were obtained as previously described (Wagner *et al*., 2002). Briefly, crude extracts obtained as above were centrifuged at 35.000 *xg* for 20 min, and the resulting supernatant ($S_{35,000\ xg}$) was then re-centrifuged at 100.000 *xg* (Beckman, rotor TY65) for 1 h. The P100.000 *xg* pellet was then resuspended in a buffer containing Tris-HCl 10 mM pH 7.4, 1 mM PMSF +1 tablet PIM, 0.5% IGEPAL CA-630 and 0.007% Triton X-100 to solubilize the membranes. All steps were carried out at 4°C and protein concentration was estimated by the Bradford assay as previously described (Wagner *et al*., 2002).

Co-immunoprecipitation experiments, Western blotting and IP analysis were performed as previously described (Wagner *et al*., 2002) by using 1.5–2.5 mg of crude extracts. Briefly, the IP reactions were incubated in an 1× IP buffer [50 mM potassium phosphate pH 7.6, 10 mM Tris-HCl pH 7.4, 1 mM EDTA pH 8, 0.007% Triton X-100 containing 0.5% IGEPAL CA-630 (Sigma), 1 mM PMSF, 1 tablet protease inhibitor mix (Roche)], to which the antibody specified in the text was added. Typically 10 µl of anti-GFP (Roche), anti-HA (Covance) or anti-HIS (Roche) antibody were used per IP reaction or no antibody was added. In the experiments in which 5 mM GTP, 5 mM GTPγS or 5 mM GDP were used, these compounds were added to the IP reaction together with the antibody. After 3 h incubation at 4°C with rotation, 5 mg of Protein A Sepharose™ CL-4B beads (Amersham) was added and the mixture was further incubated overnight with mixing. The IP pellets were then washed at least three times with 1× IP buffer, resuspended in SDS-loading buffer and boiled.

SDS-PAGE, immunoblot analyses and ECL detection (SuperSignal® system, Pierce) were carried out as previously described (Wagner *et al*., 2002). The anti-Myo2p and anti-Sec4p were kindly provided by L.S. Weisman and D. Gallwitz, respectively, and used at a dilution of 1:1000. Anti-Mlc1p was obtained from rabbits immunized with *E. coli*-purified HIS-tagged full-length Mlc1p expressed from pET15 plasmid (Novagen). After affinity purification against the same protein, the αMlc1p antibody was used at 1:1000 dilution for Western blotting. Acquisition of chemiluminescence images obtained from the immunoblot was performed by using the KODAK Electrophoresis Documentation and Analysis System 290 (EDAS 290), and the KODAK 1D Image analysis software was used for quantification analysis. At least two images were analysed per experiment and the mean data were then plotted on a graph by using Microsoft Excel spreadsheet.

Silver staining for mass spectrometry was carried out according to Schevchenko *et al*. (1996) as described in http://www.univie.ac.at/ibmz/Mass/guidelines.htm.

Mass spectrometry and MALDI-TOF analysis

Silver-stained protein bands were excised from SDS-polyacrylamide gel supports; cysteines were reduced and alkylated with iodoacetammide (Mortz *et al*., 2001). The samples were then digested with porcine trypsin (Promega) in 40 mM ammonium bicarbonate at 37°C for 16–18 h. The reaction was stopped by freezing. Tryptic peptides were extracted by ZipTip C18 (Millipore) reverse phase material and directly eluted and crystallized in a 50% acetonitrile/water (v/v) saturated solution of a-cyano-4-hydroxycinnamic acid.

MALDI-TOF mass spectra were recorded in the positive ion mode with delayed extraction on a Reflex IV time-of-flight instrument equipped with a MTP multiprobe inlet and a 337 nm nitrogen laser. Mass spectra were obtained by averaging 100–300 individual laser shots.

Database searches with the peptide masses were performed against the NCBI non-redundant database using the peptide search algorithm MASCOT (Matrix Science) resident on a local cluster. Masses corresponding to keratin tryptic fragments or evaluated as environmental contaminants by specific blank controls were not considered in such analyses.

Fluorescent microscopy analysis

Strains *K699*, *sec2-59* and *sec18-1* expressing GFPMlc1p from pUG34 were grown at 25°C to $OD_{600} = 0.6–0.8$ and then shifted to pre-warmed media at 37°C for 1 h and 30 min. Images were collected at $t = 0$ and $t = 1.5$ h at different focal planes to allow the visualization of the GFPMlc1p rings when present. A Nikon microscope (Eclipse TE2000-U) equipped with a Plan Neofluor 60X, NA1.4, oil immersion objective, filter sets for fluorescein isothiocyanate (FITC; GFP pictures), CFP, YFP, rhodamine, differential interference contrast (DIC) optics, a HBO 100 W UV lamp (Osram) and a cooled colour camera (DS-5Mc-U1) was used. Microscope and camera were controlled by the Metamorph software. Pictures were processed with Photoshop 8.0.1 (Adobe Systems).

Acknowledgements

We thank X.-D. Gao and E. Bi for the gift of plasmids, L.S. Weisman and D. Gallwitz for the gift of antibodies; Edina Csaszar (Mass Spectrometry section Vienna University Campus, A.) for technical suggestion on mass spectrometry

and MS analysis of silver-stained samples, C. Capo for technical assistence; G. Ammerer, K. Nasmyth, W. Wagner and C. Wilson for useful discussion, C. Wilson for critical reading of the manuscript; G. Rotilio and G. Federici for constant support. This work was supported by a grant from the Telethon Foundation-Italy. Pamela Bielli was supported by a fellowship from the Foundation 'Institut Patsteur-Cenci Bolognetti'.

References

Aiyar, A., Xiang, Y., and Leis, J. (1996) Site-directed mutagenesis using overlap extension PCR. *Methods Mol Biol* **57:** 177–191.

Bahler, M., and Rhoads, A. (2002) Calmodulin signaling via the IQ motif. *FEBS Lett* **513:** 107–113.

Bialek-Wyrzykowska, U., Bauer, B.E., Wagner, W., Kohlwein, S.D., Schweyen, R.J., and Ragnini, A. (2000) Low levels of Ypt protein prenylation cause vesicle polarization defects and thermosensitive growth that can be suppressed by genes involved in cell wall maintenance. *Mol Microbiol* **35:** 1295–1311.

Boyne, J.R., Yosuf, H.M., Bieganowski, P., Brenner, C., and Price, C. (2000) Yeast myosin light chain, Mlc1p, interacts with both IQGAP and class II myosin to effect cytokinesis. *J Cell Sci* **113:** 4533–4543.

Catlett, N.L., Duex, J.E., and Weisman, L.S. (2000) Two distinct regions in a yeast myosin-V tail domain are required for the movement of different cargoes. *J Cell Biol* **150:** 513–526.

Chen, S.H., Chen, S., Tokarev, A.A., Liu, F., Jedd, G., and Segev, N. (2005) Ypt31/32 GTPases and their novel F-box effector protein Rcy1 regulate protein recycling. *Mol Biol Cell* **16:** 178–192.

Collins, R.N., Brennwald, P., Garrett, M., Lauring, A., and Novick, P. (1997) Interactions of nucleotide release factor Dss4p with Sec4p in the post-Golgi secretory pathway of yeast. *J Biol Chem* **272:** 18281–18289.

Elkind, N.B., Walch-Solimena, C., and Novick, P.J. (2000) The role of the COOH terminus of Sec2p in the transport of post-Golgi vesicles. *J Cell Biol* **149:** 95–110.

Fehrenbacher, K.L., Boldogh, I.R., and Pon, L.A. (2003) Taking the A-train: actin-based force generators and organelle targeting. *Trends Cell Biol* **13:** 472–477.

Feig, L.A. (1999) Tools of the trade: use of dominant-inhibitory mutants of Ras-family GTPases. *Nat Cell Biol* **1:** 25–27.

Fielding, A.B., Schonteich, E., Matheson, J., Wilson, G., Yu, X., Hickson, G.R., *et al.* (2005) Rab11-FIP3 and FIP4 interact with Arf6 and the exocyst to control membrane traffic in cytokinesis. *EMBO J* **24:** 3389–3399.

Gao, X.D., Albert, S., Tcheperegine, S.E., Burd, C.G., Gallwitz, D., and Bi, E. (2003) The GAP activity of Msb3p and Msb4p for the Rab GTPase Sec4p is required for efficient exocytosis and actin organization. *J Cell Biol* **162:** 635–646.

Goud, B. (2002) How Rab proteins link motors to membranes. *Nat Cell Biol* **4:** 77–78.

Graham, T.R., and Emr, S.D. (1991) Compartmental organization of Golgi-specific protein modification and vacuolar protein sorting events defined in a yeast *sec18* (NSF) mutant. *J Cell Biol* **114:** 207–218.

Grote, E., and Novick, P.J. (1999) Promiscuity in Rab–SNARE interactions. *Mol Biol Cell* **10:** 4149–4161.

Grote, E., Carr, C.M., and Novick, P.J. (2000) Ordering the final events in yeast exocytosis. *J Cell Biol* **151:** 439–452.

Hales, C.M., Vaerman, J.P., and Goldenring, J.R. (2002) Rab11 family interacting protein 2 associates with Myosin Vb and regulates plasma membrane recycling. *J Biol Chem* **277:** 50415–50421.

Jedd, G., Mulholland, J., and Segev, N. (1997) Two new Ypt GTPases are required for exit from the yeast *trans*-Golgi compartment. *J Cell Biol* **137:** 563–580.

Johnston, G.C., Prendergast, J.A., and Singer, R.A. (1991) The *Saccharomyces cerevisiae MYO2* gene encodes an essential myosin for vectorial transport of vesicles. *J Cell Biol* **113:** 539–551.

Krementsov, D.N., Krementsova, E.B., and Trybus, K.M. (2004) Myosin V: regulation by calcium, calmodulin, and the tail domain. *J Cell Biol* **164:** 877–886.

Lew, D.J. (2000) Cell-cycle checkpoints that ensure coordination between nuclear and cytoplasmic events in *Saccharomyces cerevisiae*. *Curr Opin Genet Dev* **10:** 47–53.

Li, X.D., Mabuchi, K., Ikebe, R., and Ikebe, M. (2004) Ca^{2+}-induced activation of ATPase activity of myosin Va is accompanied with a large conformational change. *Biochem Biophys Res Commun* **315:** 538–545.

Li, Y., Takagi, Y., Jiang, Y., Tokunaga, M., Erdjument-Bromage, H., Tempst, P., and Kornberg, R.D. (2001) A multiprotein complex that interacts with RNA polymerase II elongator. *J Biol Chem* **276:** 29628–29631.

Luo, J., Vallen, E.A., Dravis, C., Tcheperegine, S.E., Drees, B., and Bi, E. (2004) Identification and functional analysis of the essential and regulatory light chains of the only type II myosin Myo1p in *Saccharomyces cerevisiae*. *J Cell Biol* **165:** 843–855.

May, K.M., Watts, F.Z., Jones, N., and Hyams, J.S. (1997) Type II myosin involved in cytokinesis in the fission yeast, *Schizosaccharomyces pombe*. *Cell Motil Cytoskeleton* **38:** 385–396.

McCollum, D., Balasubramanian, M.K., Pelcher, L.E., Hemmingsen, S.M., and Gould, K.L. (1995) *Schizosaccharomyces pombe cdc4+* gene encodes a novel EF-hand protein essential for cytokinesis. *J Cell Biol* **130:** 651–660.

Miaczynska, M., Lorenzetti, S., Bialek, U., Benito-Moreno, R.M., Schweyen, R.J., and Ragnini, A. (1997) The yeast Rab escort protein binds intracellular membranes *in vivo* and *in vitro*. *J Biol Chem* **272:** 16972–16977.

Mortz, E., Krogh, T.N., Vorum, H., and Gorg, A. (2001) Improved silver staining protocols for high sensitivity protein identification using matrix-assisted laser desorption/ionization-time of flight analysis. *Proteomics* **1:** 1359–1363.

Mulholland, J., Wesp, A., Riezman, H., and Botstein, D. (1997) Yeast actin cytoskeleton mutants accumulate a new class of Golgi-derived secretary vesicle. *Mol Biol Cell* **8:** 1481–1499.

Ortiz, D., Medkova, M., Walch-Solimena, C., and Novick, P. (2002) Ypt32 recruits the Sec4p guanine nucleotide exchange factor, Sec2p, to secretory vesicles; evidence for a Rab cascade in yeast. *J Cell Biol* **157:** 1005–1015.

Otero, G., Fellows, J., Li, Y., de Bizemont, T., Dirac, A.M., Gustafsson, C.M., *et al.* (1999) Elongator, a multisubunit component of a novel RNA polymerase II holoenzyme for transcriptional elongation. *Mol Cell* **3:** 109–118.

Pfeffer, S.R., Dirac-Svejstrup, A.B., and Soldati, T. (1995) Rab GDP dissociation inhibitor: putting rab GTPases in the right place. *J Biol Chem* **270:** 17057–17059.

Pruyne, D., Legesse-Miller, A., Gao, L., Dong, Y., and Bretscher, A. (2004) Mechanisms of polarized growth and organelle segregation in yeast. *Annu Rev Cell Dev Biol* **20:** 559–591.

Rahl, P.B., Chen, C.Z., and Collins, R.N. (2005) Elp1p, the yeast homolog of the FD disease syndrome protein, negatively regulates exocytosis independently of transcriptional elongation. *Mol Cell* **17:** 841–853.

Reck-Peterson, S.L., Novick, P.J., and Mooseker, M.S. (1999) The tail of a yeast class V myosin, myo2p, functions as a localization domain. *Mol Biol Cell* **10:** 1001–1017.

Schevchenko, A., Wilm, M., Vorm, O., and Mann, M. (1996) Mass spectrometric sequencing of proteins from silver-stained polyacrylamaide gels. *Electrophoresis* **68:** 850–858.

Schott, D., Ho, J., Pruyne, D., and Bretscher, A. (1999) The COOH-terminal domain of Myo2p, a yeast myosin V, has a direct role in secretory vesicle targeting. *J Cell Biol* **147:** 791–808.

Schott, D.H., Collins, R.N., and Bretscher, A. (2002) Secretory vesicle transport velocity in living cells depends on the myosin-V lever arm length. *J Cell Biol* **156:** 35–40.

Seabra, M.C., and Coudrier, E. (2004) Rab GTPases and myosin motors in organelle motility. *Traffic* **5:** 393–399.

Shannon, K.B., and Li, R. (2000) A myosin light chain mediates the localization of the budding yeast IQGAP-like protein during contractile ring formation. *Curr Biol* **10:** 727–730.

Stevens, R.C., and Davis, T.N. (1998) Mlc1p is a light chain for the unconventional myosin Myo2p in *Saccharomyces cerevisiae*. *J Cell Biol* **142:** 711–722.

Terrak, M., Wu, G., Stafford, W.F., Lu, R.C., and Dominguez, R. (2003) Two distinct myosin light chain structures are induced by specific variations within the bound IQ motifs-functional implications. *EMBO J* **22:** 362–371.

VerPlank L., and Li R. (2005) Cell cycle-regulated trafficking of Chs2 controls actomyosin ring stability during cytokinesis. *Mol Biol Cell* **16:** 2529–2543.

Wagner, W., Bielli, P., Wacha, S., and Ragnini-Wilson, A. (2002) Mlc1p promotes septum closure during cytokinesis via the IQ motifs of the vesicle motor Myo2p. *EMBO J* **21:** 6397–6408.

Walch-Solimena, C., Collins, R.N., and Novick, P.J. (1997) Sec2p mediates nucleotide exchange on Sec4p and is involved in polarised delivery of post-Golgi vesicles. *J Cell Biol* **137:** 1495–1509.

Walworth, N.C., Goud, B., Kabcenell, A.K., and Novick, P.J. (1989) Mutational analysis of SEC4 suggests a cyclical mechanism for the regulation of vesicular traffic. *EMBO J* **8:** 1685–1693.

Wang, F., Thirumurugan, K., Stafford, W.F., Hammer, J.A., 3rd, Knight, P.J., and Sellers, J.R. (2004) Regulated conformation of myosin V. *J Biol Chem* **279:** 2333–2336.

Wu, X.S., Rao, K., Zhang, H., Wang, F., Sellers, J.R., Matesic, L.E., *et al.* (2002) Identification of an organelle receptor for myosin-Va. *Nat Cell Biol* **4:** 271–278.

Supplementary material

The following supplementary material is available for this article online:

Fig. S1. A. Silver staining of a 6% SDS-polyacrylamide gel onto which the anti-GFP immunoprecipitates of protein extracts obtained from K699 wt cells carrying the Mlc1pUG34 (lanes Mlc1GFP) plasmid or pUG34 plasmids (lane GFP) treated with 5 mM GTP (panel GTP) or 5 mM GDP (panel GDP) were loaded. The position of IgG and of GFPMlc1p is indicated.

B. Silver staining of 6% SDS-polyacrylamide gel onto which the anti-GFP immunoprecipitates from protein extracts of wt cells carrying Mlc1pUG34 (lanes GFP Mlc1) or the pUG34 (lane GFP) and treated with 5 mM GTP (panel GTP) or 5 mM GTPγS (panel GTPγS) were loaded. The position of IgG and of GFPMlc1p is indicated.

C. Quantification of αMyo2p immunoblot analysis shown in Fig. 1C.

Fig. S2. Peptide coverage and monoisotopic mass list recorded by MS-MALDI-TOF analysis from the tryptic digestion of bands shown in Fig. 2 of the text.

Fig. S3. A. Silver staining of the IP reactions obtained with α-GFP from 5 mM GTP-treated cell extracts expressing GFPMlc1p from pUG34 plasmid of wt (K699), *sec2-59* (AR9-13A) or *sec2-59* (AR9-13A) expressing HA-Sec2p from pVTU plasmid.

B. Silver staining of the IP reactions obtained with αGFP from 5 mM GTP-treated cell extracts of wt cells (K699), *sec2-59* (AR9-13A) or *sec18*-1 (RSY271) expressing GFP-Mlc1p from pUG34 plasmid. Prior cell extract preparation culture cells were treated as in (A).

Table S1. Oligonucleotide primers used for cloning, tagging and site-directed mutagenesis.

This material is available as part of the online article from http://www.blackwell-synergy.com